OXFORD

SOT | Society of Toxicology
www.toxsci.oxfordjournals.org

TOXICOLOGICAL SCIENCES, 149(2), 2016, 277–288

doi: 10.1093/toxsci/kfv234
Advance Access Publication Date: October 30, 2015
Research Article

Elevated Lifetime Lead Exposure Impedes Osteoclast Activity and Produces an Increase in Bone Mass in Adolescent Mice

Eric E. Beier,*,† Jonathan D. Holz,*,†,‡ Tzong-Jen Sheu,* and J. Edward Puzas*,†,1

*Center for Musculoskeletal Research; †Department of Environmental Medicine, University of Rochester School of Medicine and Dentistry, Rochester, 14624; and ‡Department of Math and Natural Sciences, D'Youville College, Buffalo, New York, 14201

[1]To whom correspondence should be addressed at Center for Musculoskeletal Research, 601 Elmwood Avenue, Rochester, New York 14642, USA. Fax: (585) 756-4727. E-mail: edward_puzas@urmc.rochester.edu

ABSTRACT

The heavy metal lead (Pb) has a deleterious effect on skeletal health. Because bone mass is maintained through a balance of bone formation and resorption, it is important to understand the effect of Pb levels on osteoblastic and osteoclastic activity. Pb exposure is associated with low bone mass in animal models and human populations; however, the correlation between Pb dosing and corresponding bone mass has been poorly explored. Thus, mice were exposed to increasing Pb and at higher levels (500 ppm), there was unexpectedly an increase in femur-tibial bone mass by 3 months of age. This is contrary to several studies alluded to earlier. Increased bone volume (BV) was accompanied by a significant increase in cortical thickness of the femur and trabecular bone that extended beyond the epiphyseal area into the marrow cavity. Subsequent evaluations revealed an increase in osteoclast numbers with high Pb exposure, but a deficiency in osteoclastic activity. These findings were substantiated by observed increases in levels of the resorption-altering hormones calcitonin and estrogen. In addition we found that pro-osteoclastic nuclear factor-kappa beta (NF-κB) pathway activity was dose dependently elevated with Pb, both *in vivo* and *in vitro*. However, the ability of osteoclasts to resorb bone was depressed in the presence of Pb in media and within test bone wafers. These findings indicate that exposure to high Pb levels disrupts early life bone accrual that may involve a disruption of osteoclast activity. This study accentuates the dose dependent variation in Pb exposure and consequent effects on skeletal health.

Key words: Pb; osteoclast; bone turnover; bone density; NF-kappa B

Despite the attempts made to decrease the amount of lead (Pb) in the environment, it remains a pervasive toxicant affecting numerous biological systems. Developmental and lifelong low-level Pb exposures are recognized as having a persistent negative impact on human health (Goyer, 1993; Jakubowski, 2011). Recent clinical and basic science reports have suggested that Pb has a profound influence on both growing and adult bone health, and furthermore has correlated Pb exposure with increased fracture risk and predisposition to bone disease (Ignasiak *et al.*, 2006; Jackson *et al.*, 2010; Khalil *et al.*, 2008).

The effect of cumulative Pb exposure is still poorly understood, specifically in the mineralized compartment of bone. Reports in animals (Bagchi and Preuss, 2005; Escribano *et al.*, 1997; Gruber *et al.*, 1997) and humans (Campbell and Auinger, 2007; Khalil *et al.*, 2008; Nash *et al.*, 2004) associate a detrimental impact of cumulative Pb burden on bone mineral density (BMD) and development of osteopenia. However, reports of Pb and bone mass are not universal in their findings. A study published by Campbell *et al.* (2004) uncovered that adolescent children with high blood Pb levels (BLL), 23.6 μg/dl, produced greater BMD measurements in vertebrae bodies and femoral heads than their low blood Pb cohort (6.5 μg/dl BLL). This discrepancy in BMD has not been well defined or characterized, and leaves the possibility that Pb may act through more than one mechanism

to influence bone processes relative to different exposure duration or level.

Pb intoxication can directly and indirectly perturb many cellular functions of bone cells. At a hormonal level, Pb concentrations between 15 and 47 μg/dl BLL may alter circulating levels of bone-responsive molecules particularly calcitonin, 1,25-dihydroxyvitamin D3, or parathyroid hormone, which direct rates of bone formation and resorption (Pounds *et al.*, 1991; Rosen *et al.*, 1980; Yuan *et al.*, 2014). These hormonal changes have been corroborated in various clinical studies, yet functional significance of relative changes with Pb has not been established. These hormones direct the mineral matrix resorbing osteoclasts, which are derived from macrophages, to fuse under specific conditions into multinucleated giant cells (Anderson, 2000). Several proteins have been characterized as essential mediators of the fusion process, including E-cadherin, DC-STAMP, and CD47 (Han *et al.*, 2000; Van den Bossche *et al.*, 2009; Yagi *et al.*, 2005). The direct influence of Pb on these pathways is largely unexplored, and furthermore the significance of observations to human exposure is not correlated.

Receptor activator of NF-κB ligand (RANKL) is the central molecular signal for macrophages to differentiate into osteoclasts by triggering production of high quantities of the enzyme tartrate-resistant acid phosphatase (TRAP) (Arai *et al.*, 1999). This process is also dependent on signals from the cytoplasmic nuclear factor of activated T-cells (NFATc1) and NF-κB pathways (Yamashita *et al.*, 2007). RANKL can activate NF-κB by several means (Hoffmann and Baltimore, 2006). The canonical pathway involves the NF-κB essential modulator-dependent activation of IκB kinase 2, which in turn phosphorylates inhibitors of κB for proteosomal degradation. This allows for translocation of the classic NF-κB dimer composed of p50 and p65/RelA. Therefore, the kinetics for pathway activation are rapid as it avoids new biological synthesis. There are overlapping functions of NF-κB signaling proteins, as evidenced by only ablation of p50 and p52 produce an osteopetrosis from a defect in osteoclastogenesis (Iotsova *et al.*, 1997). Pb has been shown to activate NF-κB (Korashy and El-Kadi, 2008; Kudrin, 2000; Liu *et al.*, 2012), but its role in the RANKL-mediated osteoclast formation is unexplored.

In this study, we provide evidence that elevated levels of Pb, early in life, produces a deficiency in osteoclastic activity, thus elevating bone mass through an inability of osteoclasts to remodel bone. These effects may explain our observations that high Pb exposure increases BMD, but results in aberration of bone structure.

MATERIALS AND METHODS

Animal care and Pb exposure. We randomly split timed pregnant C57Bl/6 mice (Jackson Labs) to receive water containing 0 ppm Pb (0 Pb), 200 ppm Pb, or 500 ppm Pb acetate starting at delivery of litters. Male and female offspring were continued on Pb-treated water following weaning at 21 days until sacrifice to mimic lifetime exposure. All animals were housed on a 12-h light/dark cycle and had access to water and food *ad libitum*. All protocols and procedures involving animals were approved by our institution's IACUC.

BLLs were monitored by subcutaneous bleeds at 1, 3, 6, and 12 months of age and were analyzed by anodic stripping voltammetry using the Lead Care II system (Magellan Diagnostics). For determination of bone Pb, proximal halves of tibiae were isolated and marrow cavities were flushed with phosphate-buffered saline. Bones were further incubated in 3% hydrogen peroxide for 20 min to remove all marrow elements and blood cells. Then, bones were processed as described in Parsons (1993) and analyzed using atomic absorption spectroscopy.

Serum bone remodeling markers. We measured the bone formation markers amino-terminal type 1 procollagen (P1NP: Nordic Biosciences) in blood serum using ELISA kits according to the manufacturer's instructions. The bone resorption marker C-terminal telopeptide (CTx-1 RatLaps: Nordic Biosciences), osteoclast marker TRAP5b (Nordic Biosciences), RANKL (Abcam), and osteoprotegerin (OPG: R&D Systems) were measured using standard ELISA methods. Also, serum amounts of 17β-estradiol (Abcam), dickoff-1 (DKK-1: R&D Systems), and calcitonin (ALPCO) were analyzed using standard ELISA methods.

Imaging: radiography, bone densitometry, and micro-computed tomography. We obtained radiographic images of vertebrae and femur-tibia regions using a Faxitron cabinet X-ray system. The areal BMD (aBMD) were determined from harvested mice *ex vivo* by DXA (Lunar Prodigy Advance; GE Healthcare). The region of interest (ROI) included the lumbar vertebrae (LV1–LV5) and femur-tibia (entire femur in addition to the part of tibia above tibia/fibular junction) as previously described in Kostenuik *et al.* (2001). Subsequent proportions of body fat mass and bone mass were also measured using DXA. Femur length was determined from greater trochanter to medial condyle and femur diameter at the midshaft using a mechanical sliding caliper.

Mouse femurs, tibia, and lumbar vertebra (LV4) were imaged by micro-computed tomography (microCT) (VivaCT40, Scanco Medical) using a 10.5 μm resolution, 55 KVp, 142 μAmp multi-slice cone beam as described in Guo *et al.* (2008). For trabecular bone a region was selected equivalent to 8% of the femur height, 1.06 mm in total, beginning 0.3 mm from the most proximal aspect of the growth plate. Bone volume fraction (BV/TV), connective density (Conn.D), trabecular number (Tb.N), trabecular thickness (Tb.Th), trabecular spacing (Tb.Sp), structural model index (SMI), and anisotropy were determined using Scanco's 3D analysis tools (direct model). SMI is a method for determining the geometry of trabecular contours and anisotropy is a measure of directionality dependence of a material characteristic of its physical properties. Images were reconstructed to an isotropic voxel size of 10.3 μm. For cortical analyses, we chose a 0.315 mm region in the center of the midshafts for generation of cortical thickness (Cort Th) and bone area (Cort BA). For determination of the bone properties of LV4, trabecular bone in the entire vertebral body was used.

Biomechanical testing. Femoral specimens were prepared for destructive 3-point flexural tests with the anterior surface in tension using an 8-mm support span (Instron 4465/5500). Force was generated with a displacement rate of 3 mm/min. The bone parameters maximum load, stiffness, and energy absorption data were generated from the load-displacement curve for each specimen. Samples were stored frozen at −20°C, thawed to ambient temperature, and then rehydrated in PBS for 1 h before testing.

Bone histomorphometry. After harvest, mouse skeletal elements were fixed in 10% formalin for 4 days. Bones were decalcified for either 9 days in formic acid or 2 weeks in 14% EDTA, processed, and embedded in paraffin. Medial sections were obtained from specimens using a HM355S microtome (Thermo Scientific) at a thickness of 3 microns and stained with alcian blue hematoxylin (ABH) and orange G for analysis of bone properties. EDTA-decalcified samples were stained for TRAP antigen to identify osteoclasts.

Bone parameters were calculated and expressed according to published methods using Osteomeasure bone analysis software (Osteometrics) (Dempster *et al.*, 2013). The ROI for tibial trabecular bone was an area (1.23 mm^2) inferior to the growth plate within the proximal tibial metaphysis. The ROI for lumbar trabecular bone included all trabecular bone within the vertebral body. The ROI for cortical bone data collection encompassed a 2.0 mm region about the midline. For intramedullary fat analysis, the numbers of fat vacuoles in the adipose tissue within the trabecular area were counted, which appear optically empty in sections.

RNA isolation, protein isolation, and RT-PCR.. Right tibiae were isolated, the epiphyses and soft tissues were discarded, and flushed the bone marrow with a 25-gauge 5/8-in. needle. Bones were homogenized 4 per treatment group using the Tissuelyser II system (Qiagen), and either RNA using TRI Reagent (MRC Inc.) or total protein using lysate buffer (Pierce) were extracted according to the manufacturer's recommendation. Isolated RNA underwent DNase digestion and column separation using QIAGEN mini columns. Then, reverse transcription was accomplished using the iScript cDNA synthesis kit from Bio-Rad, and RT-PCR reactions were executed using PerfeCTa SYBER green (Quanta BioSciences Inc.) according to the manufacturer's protocols. The genes of interest were normalized to β-actin expression. Primer sequences are available in Supplementary Table S1.

Western blotting. Protein was fractionated into nuclear and cytoplasmic extracts using the NE-PER kit (Pierce). Protein analysis was conducted as described by Ryan *et al.* (2007). Briefly, 20 μg of isolated protein were fractionated by 10% SDS-PAGE and transferred onto nitrocellulose membranes. Membranes were blocked in 5% milk and then incubated overnight using the following antibodies: monoclonal mouse β-catenin (Santa Cruz), tumor necrosis factor alpha (TNF-α: Millipore), RelA (NF-κB p65: Santa Cruz), inhibitor of NF-κB kinase-alpha (IκK-α: Cell Signaling), or β-actin (Abcam). After washing, membranes were blotted with the appropriate secondary antibody for 1 h. Bands were visualized with enhanced chemiluminescence (Amersham Biosciences) by autoradiography film according to the manufacturer's protocol and quantified with ImageJ.

Transfection and luciferase assay. RAW264.7 cells were seeded in Dulbecco's Modified Eagle Media with 10% FBS for experimentation. Pb acetate was added to media for 8 hr, and total protein lysates was harvested for Western blotting. Luciferase activity assays were performed following transfection of RAW264.7 cells with a mixture of reporters for NF-κB (NF-κB-Luc, 1 μg) and Renilla (SV-40, 10 ng) and FuGENE HD reagent (Promega) according to protocol recommendations. We conducted transfections as described in Zuscik *et al.* (2007). Following transfection, cells were treated for 24 h with Pb, TNF-α, or the combination. Extracts were prepared using the Dual Luciferase Assay System (Promega) and tested on an Optocomp luminometer (MGM Instruments) as directed by the manufacturer.

Osteoclast formation and activity assays.. Bone marrow aspirates were seeded at 1.75×10^5 cells per well on sterile 4 × 4 mm bovine femoral cortical bone wafers. The cells were cultured in α-MEM with 10% FBS supplemented with M-CSF (30 ng/ml), RANKL (100 ng/ml), 1% l-glutamine, 1% penicillin/streptomycin, and 1% nonessential amino acids (Life Technologies). 50% medium was added the next day with the previously indicated Pb concentration, and medium was changed every other day thereafter. After 12 days, the wafers were scraped, dried, stained with toluidine blue, and examined under a 40 × objective as described in Boyan *et al.* (2003). Resorption pits were traced on the wafer surface to determine the total pitted area using Osteometrics software as described in (Childs *et al.*, 2001).

Cortical bone wafers were constructed from goat femurs that had been grazing in a field contaminated with Pb from batteries. Bone marrow cells were seeded and treated as described earlier without additional Pb treatment, and total pitted area was calculated using Osteometrics. Then, wafers were submitted for Pb analysis as described earlier.

Statistical analysis.. Results are expressed as the sample mean ± SE. One- or two-way analysis of variance followed by Tukey's multiple comparisons of means post-test was used to determine dose-dependent effects, with $P \leq .05$ used as the criteria for significance.

RESULTS

Exposure to High Pb Levels Produces Elevated BMD, Along With Decreased stature in Mice

Pb level monitoring was conducted longitudinally in soft and mineralized tissue to denote current and cumulative Pb exposure, respectively (Barbosa *et al.*, 2005). Average BLLs of female mice at 1 and 3 months of age given 200 ppm Pb was 21–24 μg/dl and 500 ppm Pb was 41–50 μg/dl (Table 1). Bone Pb levels at 3 months of age were 206 and 448 μg/g. Tibial Pb deposition was increased at 12 months compared with at 3 months in female mice, by 75.2 and 82.7%, respectively with 200 and 500 ppm Pb exposures. Bone Pb levels were 30.6% lower in 200 ppm Pb-treated male offspring compared with female littermates at 12 months (Supplementary Table S2).

Ex vivo DXA analysis was used to detect global changes in BMD. Female mice exposed to 500 ppm Pb showed no measurable difference in areal BMD in the lumbar spine LV1-LV5 at 3 months (Figure 1A). However, aBMD in the long bones, femur-tibia, was significantly increased 26.9% in mice given high-level Pb at 3 months compared with water-drinking controls (Figure 1B and C). DXA scans further revealed a relative 24.7% increase in skeletal bone weight as a contribution of total body weight in the group exposed to 500 ppm Pb, whereas the contribution of body fat to total body weight was not significantly altered (Figure 1C).

Table 1 Pb Levels in Female Mice at 1, 3, and 12 Months of Age (Blood: μg Pb/dL Whole Blood, Bone: μg Pb/g Tibial Bone).

Blood Pb	0 ppm Pb	200 ppm Pb	500 ppm Pb
1 months	0.75 ± 0.32	$23.84 \pm 2.33^{**}$	$49.89 \pm 2.89^{*,**}$
3 months	0.51 ± 0.12	$20.78 \pm 1.64^{**}$	$40.73 \pm 1.67^{*,**}$
Bone Pb			
3 months	1.82 ± 1.09	$205.5 \pm 21.14^{**}$	$448.12 \pm 20.95^{*,**}$
12 months	0.46 ± 0.10	$360.23 \pm 48.61^{**,***}$	$818.63 \pm 121.75^{*,**,***}$

Pb was measured in peripheral blood by anodic stripping voltammetry on mice treated with 0, 200, or 500 ppm Pb water ($n = 5$). Pb was measured in mineralized tissue by atomic absorption ($n = 4$). $^{*}P < .05$ for effect of Pb, $^{**}P < .05$ for multiple comparisons versus 0 Pb, $^{***}P < .05$ for multiple comparisons versus 3 months Pb.

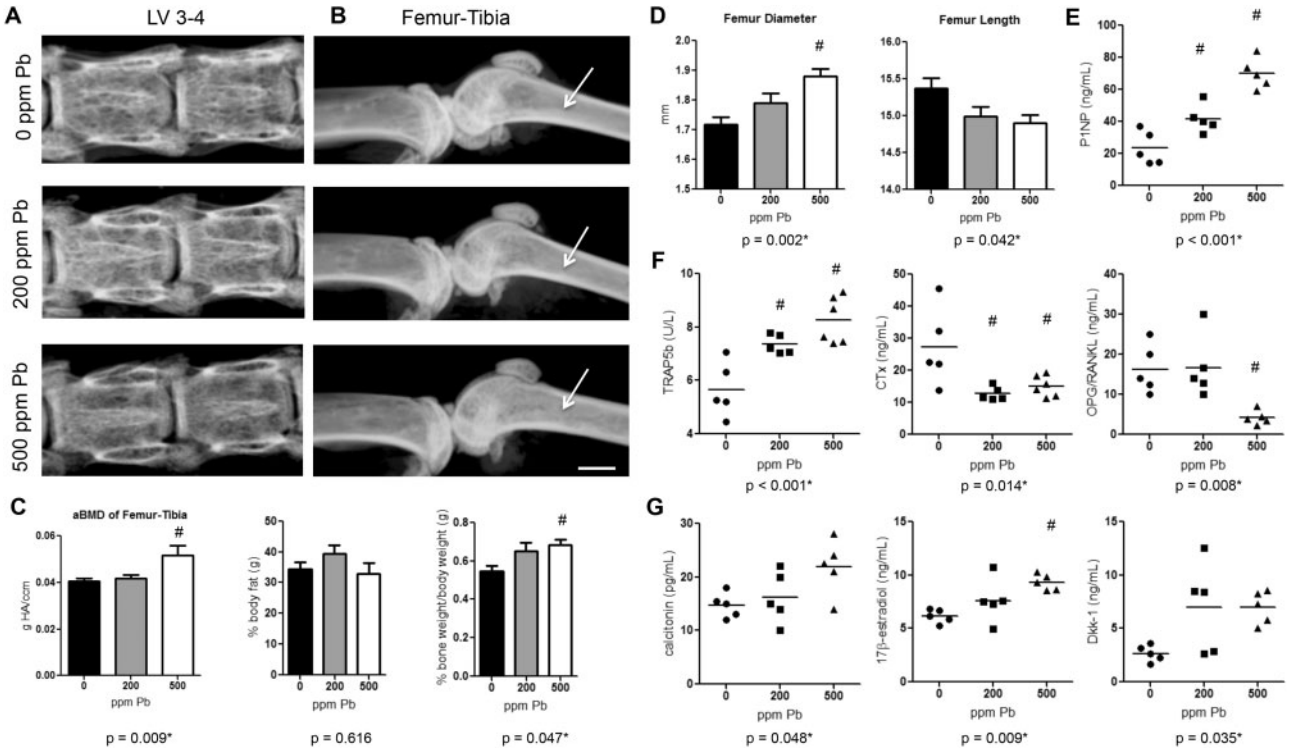

FIG. 1. Elevated Pb exposure increases BMD, distorts bone growth, and alters serum bone biomarkers in female mice. Female C57Bl/6 mice were continuously exposed to 0, 200, or 500 ppm Pb through their drinking water. Radiographic images of vertebrae (**A**) and femur-tibia (**B**) were taken *ex vivo* of each treatment group at 3 months of age. Radiolucency in the trabecular region (arrows-**B**) highlight changes in trabecular architecture. Bar: 750 μm. **C**, DXA quantification of bone mass, bone weight, and body fat is shown. **D**, Femur diameter and length were measured to determine mouse stature at 6 months. Bone formation biomarkers (**E**), bone resorption indicators (**F**), and hormones and signaling molecules (**G**) were measured using standard ELISA methods at 3 months. Data represent mean ± SEM, $n = 6$ mice/group. Scatter plots are expressed as a population spread with an average bar ($n = 5$–6/group). *$P < .05$ for effect of Pb, #$P < .05$ for multiple comparisons versus 0 Pb.

Femurs from 6-month-old female mice treated with high-level Pb were 3.1% shorter in average length, but alternatively were considerably wider in diameter, 9.6% (Figure 1D). This suggests that growth may have been stunted with Pb treatment, and bone expansion may have occurred laterally.

To determine if Pb exposure affected the balance between bone formation and bone resorption, we measured serum biomarkers of each process in 3-month-old female mice (formation Figure 1E: P1NP / resorption Figure 1F: TRAP5b, CTx-1, and OPG/RANKL/hormones and signaling molecules Figure 1G: calcitonin, estrogen, and DKK-1). Surprisingly, the procollagen molecule P1NP, an indicator of osteoblast activity, was significantly increased 3-fold with high Pb exposure over water controls. Examining the activity of the osteoclastic molecule TRAP5b indicates a 1.5-fold rise in osteoclast numbers with increasing Pb concentration compared with control mice. In contrast, the resorption activity marker CTx-1 was reduced 44.6% with increasing Pb exposure. This suggests that there was an inverse relationship between rising osteoclast numbers and functional activity of osteoclasts. The OPG/RANKL ratio depicts that as there was a 1.6-fold increase in OPG with elevated Pb exposure, yet there was a greater 4.9-fold rise in RANKL resulting in an overall significant 74.3% decrease in the OPG/RANKL in 500 ppm Pb-treated mice. Calcitonin was dose-dependently increased with elevating Pb treatment (500 ppm Pb 1.49-fold compared with 0 Pb), along with levels of 17β-estradiol (500 ppm Pb 1.51-fold compared with 0 Pb). DKK-1 levels were also elevated with increased Pb exposure (500 ppm Pb 2.63-fold compared with 0 Pb). TRAP5b and DKK-1 levels were also significantly elevated in male mice at 3 months (Supplementary Figure S1).

High Pb Exposure Produces Net Bone Gain in the Growing Adolescent Mouse Skeleton

To further examine the consequences of elevated Pb on the skeleton, quantitative microCT was conducted on femur, tibia, and vertebral bone at several time points throughout life. BV was significantly increased 2.6-fold in the femur of 500 ppm Pb-treated female mice at 6 months of age compared with control mice (Figure 2A). In addition, there was an observed dose-dependent 61.0% increase in Tb.N and 3.5-fold increase in Conn.D (Figure 2B) compared with water controls. Tb.Sp was dose-dependently decreased 38.7% in 500 ppm Pb-treated mice, while the SMI of trabeculae was significantly decreased 27.9%. These alterations in BV were significant by 3-months of age, and remained significantly different out to 12-months of age. Similar trends were observed in female tibia (Supplementary Figure S2) and in male femur, tibia, and vertebrae (Supplementary Figure S3).

Analysis at the femoral midshaft showed that Pb exposure significantly increased cortical thickness (12.3% at 200 ppm Pb and 14.8% at 500 ppm Pb) and bone area (38.7% at 500 ppm Pb) in 6-month-old female mice compared with controls (Figure 2C). Cortical thickness of lumbar vertebrae; however, was significantly decreased starting at 6 months (13.8% at 200 ppm Pb and 15.1% at 500 ppm Pb) in females compared with controls (Supplementary Figure S4). In control mice, trabecular bone normally extends 2.8 mm from the growth plate (Figure 2D). Female mice treated with Pb showed a dose-dependent increase of trabecular bone up into the midshaft region (27.4% at 200 ppm Pb and 38.2% at 500 ppm Pb).

The effect of 500 ppm Pb on the trabecular region of LV3 in female mice produced no significant change in BV (Figure 3A); however, the underlying parameters of trabecular bone were

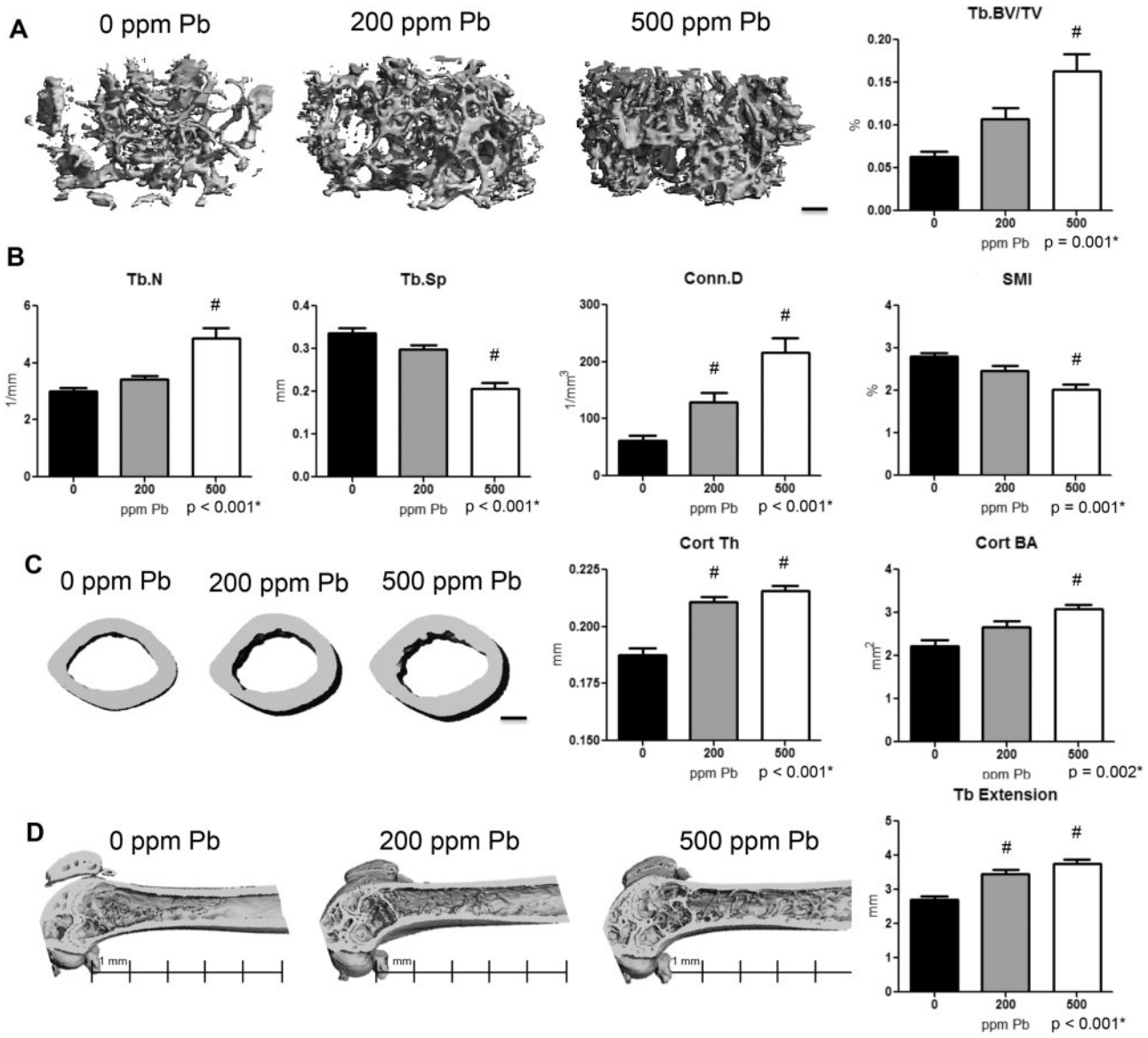

FIG. 2. Increased bone mass and cortical properties in female mice with elevated Pb exposure. **A,** Representative images (left) of transverse sections of the distal femur selected based on the median BV/TV (right) are presented at 6 months of age. **B,** Quantitative microCT determination of trabecular bone parameters and structure. **C,** Representative transverse sections of femur midshaft (left) and analysis of cortical parameters (right) including thickness and area are shown. **D,** Trabecular bone extension up the femoral midshaft was measured among groups, with a scale shown beneath representative images. Bars: 200 μm. Data represent mean ± SEM of 6 mice/group. *$P < .05$ for effect of Pb, #$P < .05$ for multiple comparisons versus 0 Pb.

significantly altered. We observed a significant 15.1% increase in trabecular number and 2.2-fold increase in connectivity in 3-month-old mice treated with 500 ppm Pb compared with controls (Figure 3B). Tb.Sp was significantly lower at all points analyzed. Trabecular shape was radically altered by elevated Pb exposure (Figure 3C). Specifically, trabecular thickness was distinctly decreased 17.3% in 500 ppm Pb-treated mice. This drastic decrease in thickness in 200 ppm Pb-treated mice could be responsible for the significant decrease observed in BV (Figure 3A). The average SMI in 6-month-old control mice was 0.6, and high-level Pb increased the average SMI to 1.8 (1.73-fold) resulting in trabeculae that were more rod-like in structure. Significant 31.8% decrease in anisotropy was found in Pb exposed mice compared with controls, suggesting that bones from high-level Pb exposure could be more susceptible to cracks and may propagate fractures.

Pb Alters Mineral and Tensile Bone Strength

Destructive 3-point bending tests were conducted to assess bone strength about the femoral midshaft. 500 ppm Pb-exposed female mice produced bones with significant increases in biomechanical metrics: 15.5% maximum stiffness, 4.8% maximum load, 60.1% energy to failure, and 85.3% post-yield energy compared with water controls in 6-month-old mice (Table 2). This may suggest a functional alteration in the material properties of bone hardness and loading capability.

To determine strength of vertebral bone, LV4 were compression tested in 6-month-old female mice. Exposure to 500 ppm Pb diminished bone strength in LV4, characterized by a significant 14.1% reduction in maximum load, 19.3% in maximum stiffness, and 23.5% in energy to failure compared with water controls (Table 2). This suggests that the changes in trabecular

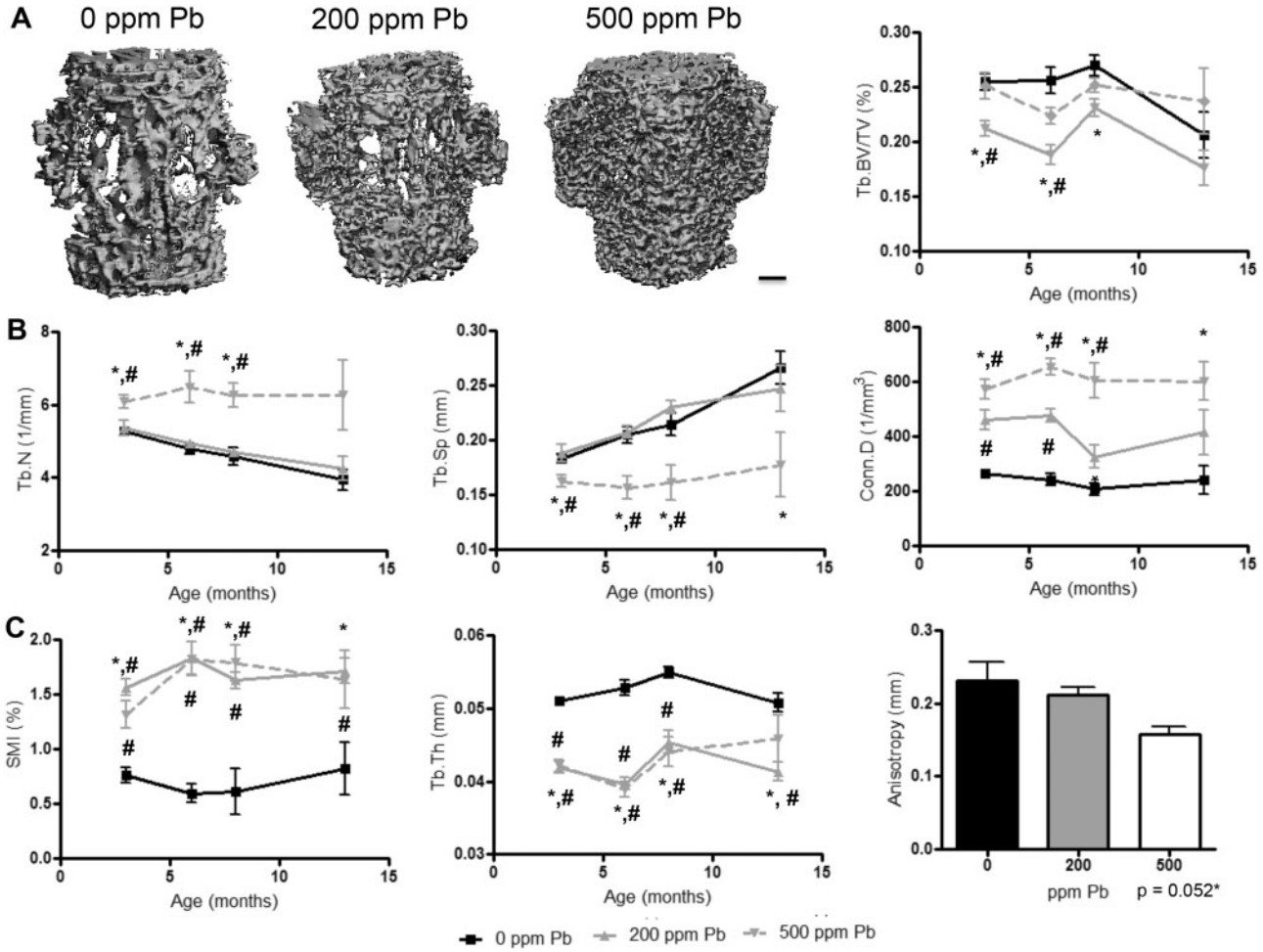

FIG. 3. Pb exposure impairs trabecular bone properties in the lumbar spine of female mice. **A**, Images are representative transverse sections of LV4 (left, bar: 200 μm) selected based on the median BV/TV (right) at 6 months. **B**, Additional microCT analyses of trabecular bone properties are provided of each group over time. **C**, Architectural measures of trabecular shape, thickness, and directionality are presented over time, and at 12 months for anisotropy. Data represent mean ± SEM of 5 mice/group. *$P < .05$ for effect of Pb, #$P < .05$ for multiple comparisons versus 0 Pb.

TABLE 2. Bone Strength Determination in Femur and Vertebrae of Pb-Treated 6-Month-Old Female Mice.

3-pt bending	Stiffness (N/mm)	Max load (N)	Energy to failure (mJ)	Post-yield energy (mJ)
0 ppm Pb	119.91 ± 2.91	15.62 ± 0.11	2.68 ± 0.18	1.91 ± 0.18
200 ppm Pb	127.22 ± 5.00	15.09 ± 0.28	2.12 ± 0.21	1.31 ± 0.31
500 ppm Pb	138.57 ± 3.86*,**	16.36 ± 0.21*,**	4.28 ± 0.27*,**	3.54 ± 0.28*,**
Compression				
0 ppm Pb	131.28 ± 5.03	16.53 ± 0.21	4.18 ± 0.23	4.19 ± 0.35
200 ppm Pb	113.22 ± 5.09**	15.60 ± 0.37	3.11 ± 0.28**	1.96 ± 0.24**
500 ppm Pb	106.23 ± 3.35*,**	14.15 ± 0.15*,**	3.20 ± 0.19*	3.69 ± 0.44*

Flexure testing was applied to mouse femurs and compression testing to LV4. Resistance to force was plotted over time and data was calculated to represent mean ± SEM for 7 mice/group, *$P < .05$ for effect of Pb, **$P < .05$ for multiple comparisons versus 0 Pb.

structure observed in Figure 3C compromised the structural integrity of the trabecular architecture.

Osteoclast and Adipocyte Numbers Are Increased With Elevated Pb Exposure

To determine the effect of Pb on bone processes, histomorphometric analyses in Pb-treated mice were conducted. Trabecular bone in the proximal tibia of 6-month-old female mice showed a consistent increase in trabecular BV/TV (34.8%) for 500 ppm Pb-treated mice compared with water controls (Figure 4A). Significant elevation of osteoclast parameters (N.Oc/Tb.Ar 54.7%, Oc.S/BS 52.1%) was observed in 500 ppm Pb-treated mice compared with water controls (Figure 4B). In 3-month-old mice, there were subtle changes in bone marrow adiposity with elevated Pb exposure. However in 6-month--old female mice, the Pb-exposed bone marrow was filled with adipocytes (Figure 4A). Adipocyte volume (3.26-fold at 200 ppm Pb and 2.63-fold at 500 ppm Pb) was significantly increased, and adipocyte size was significantly increased 1.23-fold at 200 ppm Pb.

Dynamic histomorphometry was used to assess osteoblastic function and mineral deposition in cortical bone of Pb-exposed

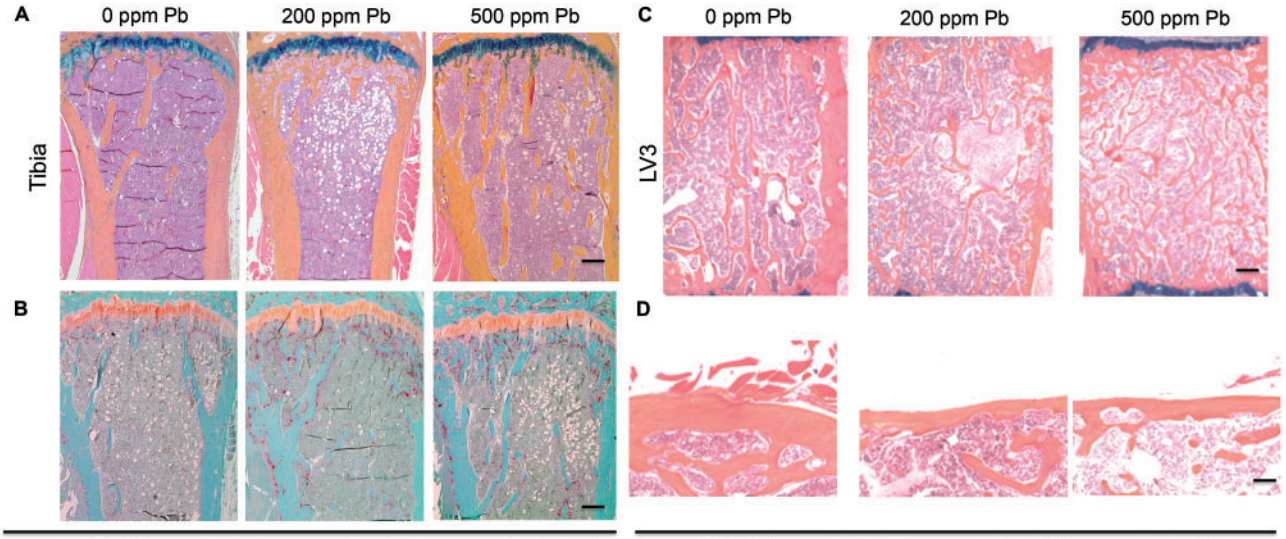

BV/TV (%)	14.0 ± 0.78	12.7 ± 0.53	18.9 ± 1.23*,#
AV/BV (%)	3.03 ± 0.65	9.88 ± 1.92#	7.95 ± 1.31*
Adip S (mm^2)	2.54 ± 0.3	3.12 ± 0.37	2.66 ± 0.44
N.Oc/Tb.Ar (mm^{-1})	115.4 ± 16.7	213.1 ± 22.1#	176.2 ± 25.4*
Oc.S/BS (%)	16.7 ± 0.7	39.3 ± 1.2#	25.4 ± 1.0*,#

BV/TV (%)	29.18 ± 2.07	23.24 ± 1.60	29.47 ± 1.41
N.Oc/Tb.Ar (mm^{-1})	181.1 ± 10.8	231.2 ± 18.5	264.6 ± 13.9*,#
Oc.S/BS (%)	35.5 ± 1.6	41.3 ± 1.7	44.6 ± 2.6*,#
Cort Th (mm)	11.7 ± 0.7	7.3 ± 0.6#	7.6 ± 0.4*,#
Cort Po. (%)	4.7 ± 0.3	7.8 ± 0.8#	8.1 ± 0.6*,#

FIG. 4. Pb exposure increases adipocyte formation and osteoclast formation, and vitiates cortical bone quality in female mice. At 6 months of age, bone specimens were stained with ABH (**A, C, D**) or TRAP (**B**). Representative images of trabecular (**A, B, C**) and cortical (**D**) bone of proximal tibias and lumbar vertebrae were selected based on the median BV/TV of each group (top). The effect of Pb on histologic parameters were calculated and displayed in the tables (bottom). Bar: (**A–C**) 100 μm, (**D**) 500 μm. Data represent mean ± SEM of 4 mice/group. *$P < .05$ for effect of Pb, #$P < .05$ for multiple comparisons versus 0 Pb.

female mice. At 6 months of age, there is little endosteal bone formation and it is mainly periosteal bone formation that regulates thickness in mouse cortices. Overall, Pb did not have a strong influence on bone formation at this time point, although trends existed indicating a non-significant elevation in bone formation rates in 500 ppm Pb and non-significant decreased in formation rates in 200 ppm Pb compared with water controls (Supplementary Figure S5).

Examination of trabecular bone in the LV3 of high-level Pb-treated female mice corroborated the results from microCT (Figure 4C). There was no change in BV/TV, but a significant increase in osteoclast parameters (N.Oc/Tb.Ar 31.5%, Oc.S/BS 24.9%) with elevated Pb compared with the water controls. There was a dose-dependent decrease of Pb on vertebral cortical bone (37.4% at 200 ppm Pb and 34.9% at 500 ppm Pb), which also resulted in an increase in cortical porosity (1.65-fold at 200 ppm Pb and 1.72-fold at 500 ppm Pb) compared with controls (Figure 4D).

Pathways Promoting Osteoclast Formation Are Increased in Pb-exposed Mice

To uncover the effects of Pb dosing on molecular pathways responsible for osteoclast and bone formation, important regulatory molecules were tested in tibial bone at 6 months. Analysis of protein expression suggests that β-catenin levels were down regulated in 200 ppm Pb-treated female mice by 82.1% (Figure 5A and B). Conversely, the expression pattern of NF-κB was increased in Pb-exposed mice, as shown by a significant 6-fold increase in the nuclear fraction of NF-κB in 500 ppm Pb compared with untreated mice. Concordantly, levels of the cytokine TNF-α were elevated 4-fold in bone following 500 ppm Pb exposure.

RNA expression data depict a similar description resulting from Pb exposure in 6 month-old female mice. Levels of *β-catenin* were reduced by 47.4% in 200 ppm Pb while *PPAR-γ* expression was significantly elevated by 2.7-fold in mice exposed to 200 ppm Pb compared with controls (Figure 5C). The osteoclast gene profile indicates an increase in osteoclast formation in the presence of Pb. The fusion molecule *CD47* was unaffected, but the osteoclast regulator *NFATc1* and *CTSK* were significantly elevated by 500 ppm Pb exposure, 2.8- and 3.2-fold, respectively, compared with controls (Figure 5D). All together, these data suggest that Pb creates an inflammatory state in bone, which also promoted down-stream osteoclastic formation.

Effects of Increasing Pb on Osteoclast Formation and Activity

To understand the effect of Pb on osteoclastic bone resorption, osteoclast activity was examined in isolated osteoclast precursors of Pb-treated female mice. Bone marrow cells from the 500 Pb-exposed mice at 6 months produced higher osteoclast numbers by 1.9-fold; however, these osteoclasts did not generate a significant rise in pit resorption area (Figure 6A). Interestingly, when Pb was supplemented in the media there was a reduction up to 68.7% by 20 μM Pb of osteoclast formation from bone marrow cells (Figure 6B). Then, resorption activity of bone marrow cells was examined on Pb-intoxicated bone wafers (Figure 6C). Osteoclast activity was reduced on average by 70.2% between the low (20 ppm Pb) and elevated (70 ppm Pb) bone wafers, indicating inhibition of osteoclast function.

Monocytes Have Elevated NF-κB Signaling Following Pb Treatment

An early origin osteoclastic precursor cell line, unaltered by osteoclastic promoting factors M-CSF or RANKL, was used to assess whether the rise in osteoclasts could be supported by increased activity of the pro-osteoclastogenic NF-κB/RANK pathway. RAW264.7 cells treated with increasing Pb through culture media for 8 h showed a dose-dependent increase in NF-κB signaling. This was characterized by a 4.4-fold increase in

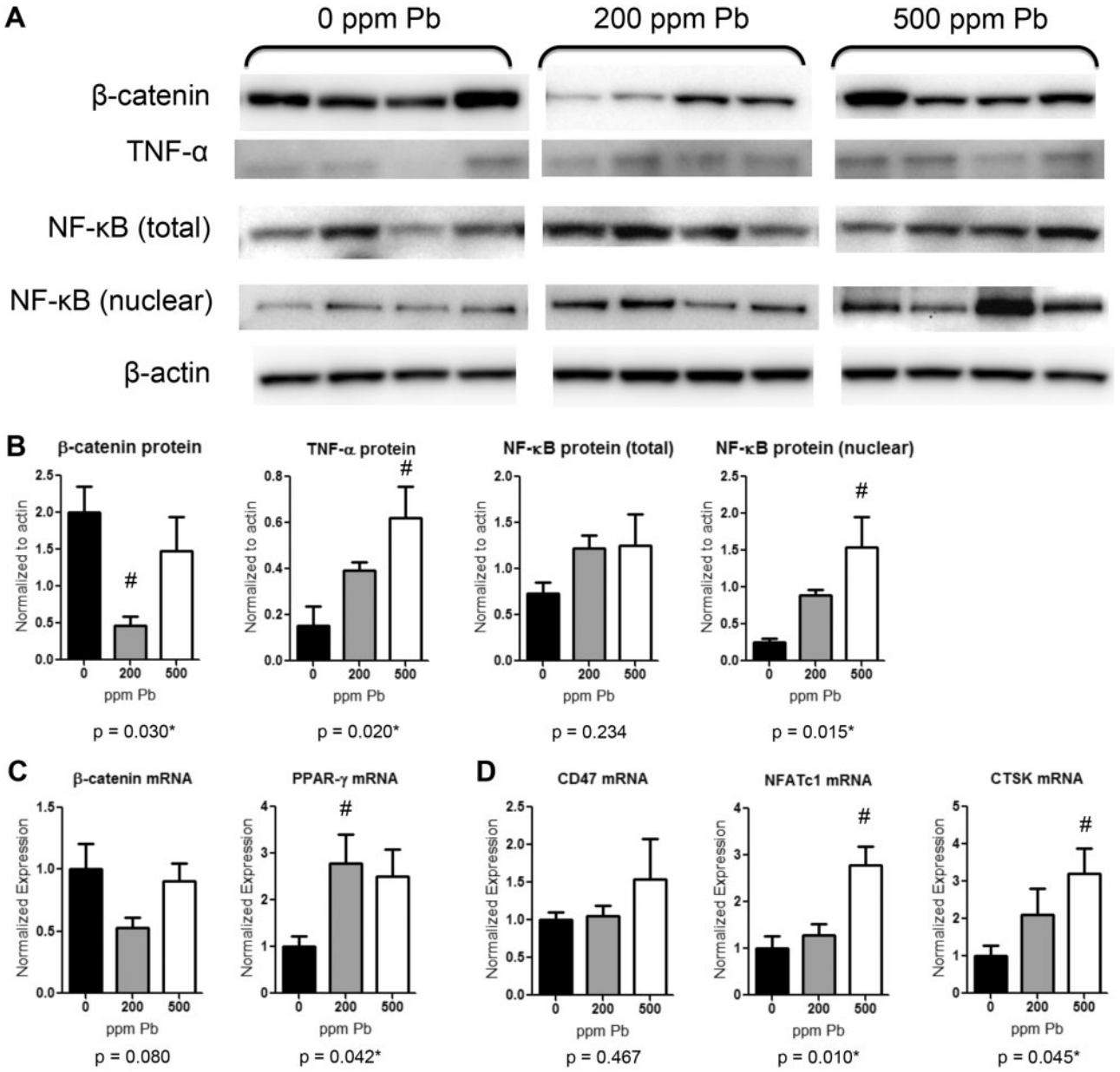

FIG. 5. Increased expression of osteogenic and adipogenic factors in bone from Pb-exposed female mice. At 6 months of age protein and RNA were isolated from tibial bone after aspiration of bone marrow cells. **A**, Western blots of β-catenin, TNF-α, NF-κB (total protein lysates and nuclear fraction), and β-actin are depicted for 4 samples from 0, 200, and 500 ppm Pb-treated mice and **B**, quantified using densitometry. **C**, *β-catenin* and *PPAR-γ* gene expression measured using RT-PCR. **D**, Osteoclastic genes *CD47*, *NFATc1*, and *CTSK* gene expression measured using RT-PCR. Data represent mean SEM ($n = 4$ mice/group). $^{*}P < .05$ for effect of Pb, $^{\#}P < .05$ for multiple comparisons versus 0 Pb.

p65 levels at 5.0 μM Pb and an inverse 84.4% decrease in IκBα levels compared with controls (Figure 6D). Similarly, NF-κB signaling on a luciferase reporter showed a 3.3-fold elevation in activity following 5.0 μM Pb exposure. TNF-α treatment increased NF-κB luciferase activity by 2.5-fold, and was further augmented in the presence of 5.0 μM Pb to 6.2-fold compared with the vehicle control (Figure 6E).

DISCUSSION

Contrary to our initial hypothesis, we found that mice given a high Pb exposure had greater BMD than unexposed control mice. Upon characterization of the bone phenotype, 500 ppm Pb treatment produced morphometric changes in bone structure and cortical parameters, generating significant changes in strength and homeostatic bone signaling. These alternations occurred early on during the Pb exposure in young mice, correlating with observations made clinically in children (Campbells *et al.*, 2004). The disruption in bone metabolism and changes in bone accrual observed here may dispose an individual to significant bone pathology later in life. This manifested in our study by severe alteration in trabecular structure and a reduction in vertebral bone strength in Pb-exposed mice.

We speculate that the observed alterations are primarily due to substantial impairment of osteoclast function. Although factors promoting osteoclast formation were elevated, such as

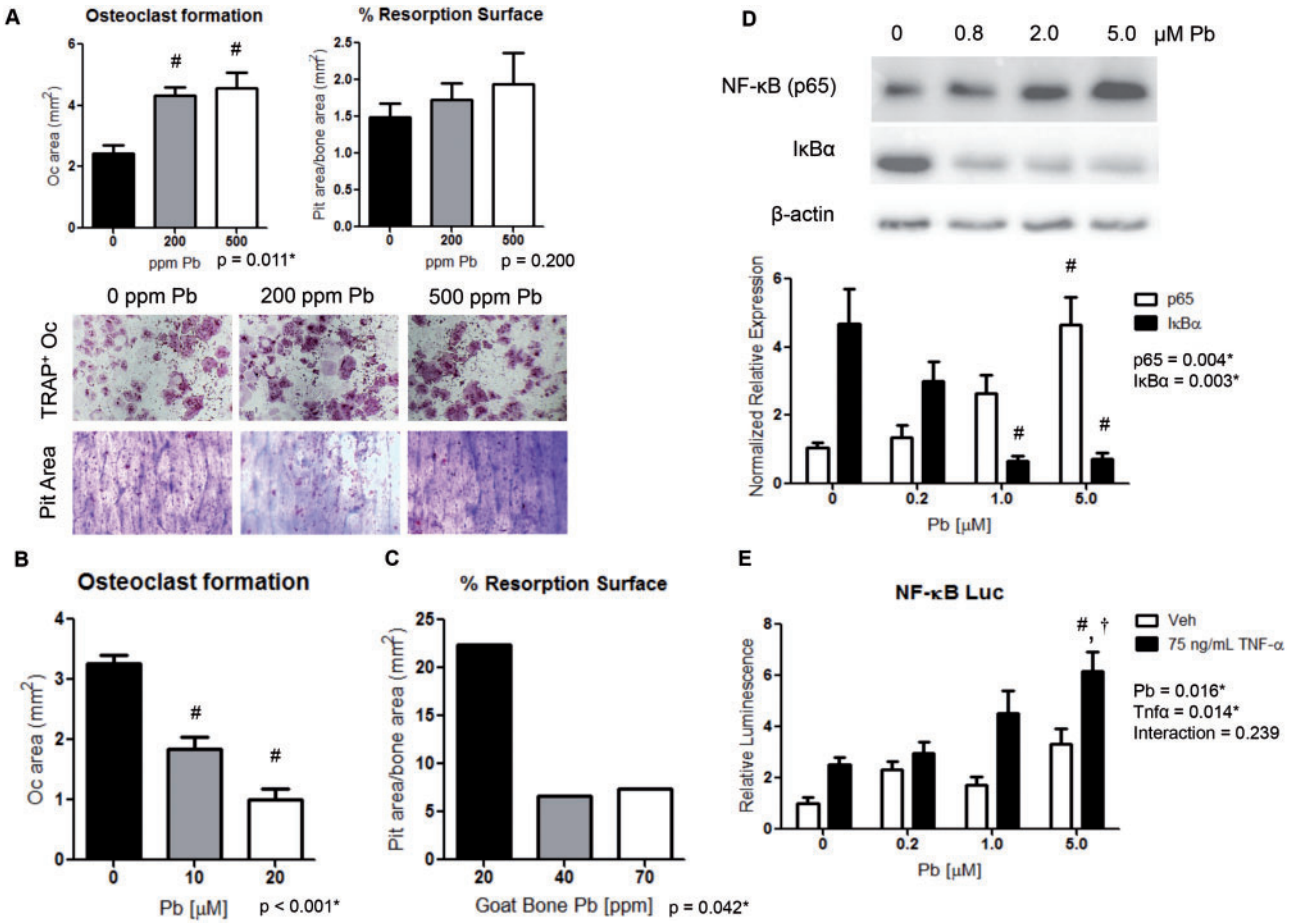

FIG. 6. Pb promotes osteoclast formation but osteoclast activity is inhibited by elevated Pb exposure. Osteoclast formation and activity was assessed on bovine cortical bone wafers. **A**, Bone marrow cells isolated from Pb-exposed mice were evaluated for TRAP+ osteoclasts and pit resorption. **B**, Osteoclastic formation was evaluated from bone marrow cells treated with Pb though the media. **C**, Pb-intoxicated bone wafers were constructed from goats and were resistant to osteoclastic resorption. NF-κB signaling was determined by Western blot (**D**) and luciferase activity (**E**) in response to increasing Pb and recombinant TNF-α in RAW264.7 cells. Data represent mean ± SEM for 3 trials. *$P < .05$ for effect of variable, #$P < .05$ for multiple comparisons versus control, †$P < .05$ for multiple comparisons versus 5 µM Pb.

increases in the NF-κB-RANKL system that corresponded with increases in osteoclast numbers histologically and systemically, bone mass was elevated with high-level Pb. This observation may be explained by a combination of several elements. (1) Pb stimulation of NF-κB in macrophage cells with matching increased TNF-α production promoted formation of osteoclasts. Increases in osteoclastic gene expression (*NFATc1* and downstream *CTSK*) were observed in bone, and may be a product of the increased number of osteoclasts, or indirect Pb action. (2) An inability of osteoclasts, in Pb-exposed mice, to resorb Pb-tainted bone produced a higher demand for osteoclasts. (3) Alterations in hormone levels modulate osteoclast activity—calcitonin directly inhibits osteoclastic bone resorption through calcitonin receptors (Eilam *et al.*, 1980) and elevated estrogen mediates osteoclast apoptosis (Hughes *et al.*, 1996). (4) Blockade of β-catenin signaling, potentially mediated by elevated DKK-1 antagonism, causes an increase in the OPG/RANKL ratio. (5) Last, increased fatty marrow is indicated to negatively influence osteoclast activity (Liu *et al.*, 2013).

The osteoclastic defect that we observed as a consequence of high Pb exposure manifested histologically by increases in trabecular number. The central core cartilage that normally exists in trabecular bone was replaced with dense and irregular bony trabeculae. One proposed mechanism for repressed osteoclast activity is the inability of resorption pit acidification whereby osteoclasts generate proton ions and pump them into the resorption area (Segovia-Silvestre *et al.*, 2009). The possible interference of an essential enzyme for this process, carbonic anhydrase, is inhibited by Pb (Ekinci *et al.*, 2007) and thus may play a role in osteoclast dysfunction. Thickened femur cortices and lesser-developed marrow cavity are observed in cases of deficient osteoclastic activity, and were consistent with our high Pb animal model.

Elevated Pb exposure produced a considerably different effect on long bones (ie, femur-tibia) compared with vertebral bone in mice. Although there was net gain in trabecular bone mass, cortical thickness, and bone strength in femurs, there was no change in trabecular bone mass in the vertebras, and decreased cortical thickness and bone strength. The reason for the disparity is unclear, yet one distinctive difference was a significant thinning of vertebral trabecular bone compared with preservation of trabecular shape in the femur. In addition, the increases in bone mass at 500 ppm were more prominent in female mice than their male cohorts, whereas some of the decreases in bone mass at 200 ppm were more apparent in the male mice. Pb is known to distribute unequally at different bones sites, and is generally greater in areas based on their approximate compact/trabecular bone ratio, showing preference for spongy bone over compact

bone (Cretacci and Parsons, 2010; Todd *et al.*, 2001; Wittmers *et al.*, 1988). Pb deposition was greater in females, and because vertebrae have a lower compact: trabecular bone ratio than tibia, we postulate that Pb deposition would be greater here. This could help explain why differences at skeletal site or by gender exist, and yet, the mechanism behind these disparities is beyond what we were able to determine here. Further investigation related to site-specific differences in bone remodeling, osteoclastic bone resorption, and bone formation capability is warranted.

These findings depart from the more traditional wisdom that Pb exposure produces a decrease in BMD. Indeed, our lab and other groups have published, mainly in rats (Bagchi and Preuss, 2005; Beier *et al.*, 2013; Escribano *et al.*, 1997; Gruber *et al.*, 1997; Hamilton and O'Flaherty, 1994), but also in mouse models (Beier *et al.*, 2015a,b; Monir *et al.*, 2010), both with subchronic and lifetime Pb exposures produce a weakening of skeletal structure. Although we did see aberrations in bone architecture and weakened vertebral bone compression strength with elevated Pb, significant gains in bone mass were observed in long bones at 3 months of age. We believe that Pb concentration and differences in bone cell susceptibility are the primary variables of concern. At chronic low dose or short duration Pb exposure osteoblastic formation is inhibited with little change in osteoclast activity (Beier *et al.*, 2013; Pounds *et al.*, 1991). However at more extreme Pb doses, 200–500 ppm Pb, osteoclastic resorption is affected at several stages of osteoclastogenesis as illustrated in this study, which overrides a decrease in bone formation. As juveniles have rapid mineral acquisition and enhanced remodeling rates than adults, there is increased prospect of augmented Pb toxicity, which subsequently is also attributed to altered growth plate formation (Gonzalez-Riola *et al.*, 1997; Hamilton and O'Flaherty, 1994) and shortened stature (Ballew *et al.*, 1999). In addition we observed indicators of increased bone formation with 500 ppm Pb. This may be related several factors including the coupling process of increased osteoclasts that secrete anabolic factors (Henriksen *et al.*, 2012), a systemic factor such as estradiol that may promote bone formation (Chow *et al.*, 1992), or accelerated growth plate fusion. Lifetime bone mass is sustained over many years in humans; therefore, it is plausible that these early gains in bone mass that occurs with high Pb may shift the overall arc of bone mass to reach a peak density earlier, and as such produce negative consequences for BMD in later years.

Elevations were found in pro-osteoclastic proteins NF-κB and TNF-α following Pb treatment, which in combination with RANKL, could support the increase we observed in osteoclastogenesis from osteoclast precursors derived from Pb-exposed female mice. *In vivo*, these osteoclasts appeared to have decreased functionality. However, when studied *ex vivo*, there was no change in activity. This is evidence for inability for osteoclasts to act on bone with high Pb composition, as well as negative hormonal regulation as essential components to the overall deficient bone turnover. This illustrates the complexity of Pb action as a promiscuous toxicant that can interfere with biological function at different levels or organ systems.

Tibial bone Pb is often used as a hallmark of cumulative Pb exposure. By 3 months, female mice exposed to 200 ppm Pb had accumulated 206 μg Pb/g bone, roughly 20–30× more than current estimates of the average human population (Ambrose *et al.*, 2000). However, compatible levels of elevated tibial Pb are reported in industrial Pb workers (Bledsoe *et al.*, 2011; Somervaille *et al.*, 1988) and in recent antiquity (Keeleyside *et al.*, 1996). The increased BMD could partially be explained by this increased Pb deposition in the skeleton. Pb is known to substitute for calcium in bone hydroxyapatite, which has been indicated to alter size, shape, and mineral properties of the structure (Bigi *et al.*, 1991). Pb is more electron dense than calcium and therefore may influence BMD measurements. Zhu *et al.* (2010) reported that high-Pb content resulted in increases in the formation of intermediate compounds of $Pb_3O_2(OH)_2$ in the $Pb(NO_3)_2{\cdot}4H_2O$, which resulted in decreased bone crystallinity.

In summary, we have presented results demonstrating alteration of bone architecture in high Pb-treated mice. This appears to be a consequence of dysfunctional osteoclastic activity, both through inhibiting osteoclast function and by rendering bone less resorbable by osteoclasts. There was evidence that Pb was able to affect the cellular environment in bone to alter the regulated state of adipocyte formation and osteoclast formation in bone marrow. We believe that this abnormal alteration in bone architecture by Pb, while producing gains in volume and BMD, created irregularities that were detrimental to overall bone health. These novel observations further our understanding of the complexities of Pb exposure, and provide explanation for the disparity in the field regarding the effect of Pb on bone structure.

FUNDING

This work was supported by the following grants from the National Institutes of Health (T32 ES07026, R01 ES012712, T32 AR053459, P01 ES011854, and P30 ES301247). Biomechanical testing was performed in the Biomechanics and Multimodal Tissue Imaging Core Laboratory, established by NIH grant (P30 AR061307).

ACKNOWLEDGMENTS

We thank Ryan Tierney and Sarah Mack for assistance with histology, Robert Gelein for bone lead measurements, and Michael Thullen for microCT imaging. We thank Maureen Newman for generation of osteoclast imaging.

REFERENCES

Ambrose, T. M., Al-Lozi, M., and Scott, M. G. (2000). Bone lead concentrations assessed by in vivo X-ray fluorescence. *Clin. Chem.* **46**(8 Pt 1), 1171–1178.

Anderson, J. M. (2000). Multinucleated giant cells. *Curr. Opin. Hematol.* **7**, 40–47.

Arai, F., Miyamoto, T., Ohneda, O., Inada, T., Sudo, T., Brasel, K., Miyata, T., Anderson, D. M., and Suda, T. (1999). Commitment and differentiation of osteoclast precursor cells by the sequential expression of c-Fms and receptor activator of nuclear factor kappaB (RANK) receptors. *J. Exp. Med.* **190**, 1741–1754.

Bagchi, D., and Preuss, H. G. (2005). Effects of acute and chronic oval exposure of lead on blood pressure and bone mineral density in rats. *J. Inorg. Biochem.* **99**, 1155–1164.

Ballew, C., Khan, L. K., Kaufmann, R., Mokdad, A., Miller, D. T., and Gunter, E. W. (1999). Blood lead concentration and childrens anthropometric dimensions in the Third National Health and Nutrition Examination Survey (NHANES III), 1988-1994. *J. Pediatrics* **134**, 623–630.

Barbosa, F., Jr., Tanus-Santos, J. E., Gerlach, R. F., and Parsons, P. J. (2005). A critical review of biomarkers used for monitoring human exposure to lead: advantages, limitations, and future needs. *Environ. Health Perspect.* **113**, 1669–1674.

Beier, E. E., Inzana, J. A., Sheu, T. J., Shu, L., Puzas, J. E., and Mooney, R. A. (2015a). Effects of combined exposure to lead and high-fat diet on bone quality in Juvenile male mice. *Environ. Health Perspect.* **123**, 935–943..

Beier, E. E., Maher, J. R., Sheu, T. J., Cory-Slechta, D. A., Berger, A. J., Zuscik, M. J., and Puzas, J. E. (2013). Heavy metal lead exposure, osteoporotic-like phenotype in an animal model, and depression of Wnt signaling. *Environ. Health Perspect.* **121**, 97–104.

Beier, E. E., Sheu, T. J., Dang, D., Holz, J. D., Ubayawardena, R., Babij, P., and Puzas, J. E. (2015b). Heavy metal ion regulation of gene expression: Mechanisms by which lead inhibits osteoblastic bone forming activity through modulation of the Wnt/beta-catenin signaling pathway. *J. Biol. Chem.* **290**, 18216–18226.

Bigi, A. Gandolfi, M., Gazzano, M., Ripamonti, A., Roveri, N., and Thomas, S. A. (1991). Structural modifications of hydroxyapatite induced by lead substitution for calcium. *J. Chem. Soc. Dalton Trans.* **11**, 2883–2886.

Bledsoe, M. L., Pinkerton, L. E., Silver, S., Deddens, J. A., and Biagini, R. E. (2011). Thyroxine and free thyroxine levels in workers occupationally exposed to inorganic lead. *Environ. Health Insights* **5**, 55–61.

Boyan, B. D., Schwartz, Z., Lohmann, C. H., Sylvia, V. L., Cochran, D. L., Dean, D. D., and Puzas, J. E. (2003). Pretreatment of bone with osteoclasts affects phenotypic expression of osteoblast-like cells. *J. Orthop. Res.* **21**, 638–647.

Campbell, J. R., and Auinger, P. (2007). The association between blood lead levels and osteoporosis among adults–results from the third national health and nutrition examination survey (NHANES III). *Environ. Health Perspect.* **115**, 1018–1022.

Campbell, J. R., Rosier, R. N., Novotny, L., and Puzas, J. E. (2004). The association between environmental lead exposure and bone density in children. *Environ. Health Perspect.* **112**, 1200–1203.

Childs, L. M., Goater, J. J., O'Keefe, R. J., and Schwarz, E. M. (2001). Efficacy of etanercept for wear debris-induced osteolysis. *J. Bone Min. Res.* **16**, 338–347.

Chow, J. W., Lean, J. M., and Chambers, T. J. (1992). 17 beta-estradiol stimulates cancellous bone formation in female rats. *Endocrinology* **130**, 3025–3032.

Cretacci, Y., and Parsons, P. J. (2010). Localized accumulation of lead within and among bones from lead-dosed goats. *Environ. Res.* **110**, 26–32.

Dempster, D. W., Compston, J. E., Drezner, M. K., Glorieux, F. H., Kanis, J. A., Malluche, H., Meunier, P. J., Ott, S. M., Recker, R. R., and Parfitt, A. M. (2013). Standardized nomenclature, symbols, and units for bone histomorphometry: A 2012 update of the report of the ASBMR Histomorphometry Nomenclature Committee. *J. Bone Min. Res.* **28**, 2–17.

Eilam, Y., Szydel, N., and Harell, A. (1980). Effects of calcitonin on transport and intracellular distribution of exchangeable Ca2+ in primary culture of bone cells. *Mol. Cell. Endocrinol.* **18**, 215–225.

Ekinci, D., Beydemir, S., and Kufrevioglu, O. I. (2007). In vitro inhibitory effects of some heavy metals on human erythrocyte carbonic anhydrases. *J. Enzyme Inhib. Med. Chem.* **22**, 745–750.

Escribano, A., Revilla, M., Hernandez, E. R., Seco, C., Gonzalez-Riola, J., Villa, L. F., and Rico, H. (1997). Effect of lead on bone development and bone mass: A morphometric, densitometric, and histomorphometric study in growing rats. *Calcif. Tissue Int.* **60**, 200–203.

Gonzalez-Riola, J., Hernandez, E. R., Escribano, A., Revilla, M., Ca, S., Villa, L. F., and Rico, H. (1997). Effect of lead on bone and cartilage in sexually mature rats: A morphometric and histomorphometry study. *Environ. Res.* **74**, 91–93.

Goyer, R. A. (1993). Lead toxicity: current concerns. *Environ. Health Perspect.* **100**, 177–187.

Gruber, H. E., Gonick, H. C., Khalil-Manesh, F., Sanchez, T. V., Motsinger, S., Meyer, M., and Sharp, C. F. (1997). Osteopenia induced by long-term, low- and high-level exposure of the adult rat to lead. *Miner. Electrolyte Metab.* **23**, 65–73.

Guo, R., Yamashita, M., Zhang, Q., Zhou, Q., Chen, D., Reynolds, D. G., Awad, H. A., Yanoso, L., Zhao, L., Schwarz, E. M., *et al.* (2008). Ubiquitin ligase Smurf1 mediates tumor necrosis factor-induced systemic bone loss by promoting proteasomal degradation of bone morphogenetic signaling proteins. *J. Biol. Chem.* **283**, 23084–23092.

Hamilton, J. D., and O'Flaherty, E. J. (1994). Effects of lead exposure on skeletal development in rats. *Fundam. Appl. Toxicol.* **22**, 594–604.

Han, X., Sterling, H., Chen, Y., Saginario, C., Brown, E. J., Frazier, W. A., Lindberg, F. P., and Vignery, A. (2000). CD47, a ligand for the macrophage fusion receptor, participates in macrophage multinucleation. *J. Biol. Chem.* **275**, 37984–37992.

Henriksen, K., Andreassen, K. V., Thudium, C. S., Gudmann, K. N., Moscatelli, I., Cruger-Hansen, C. E., Schulz, A. S., Dziegiel, M. H., Richter, J., Karsdal, M. A., *et al.* (2012). A specific subtype of osteoclasts secretes factors inducing nodule formation by osteoblasts. *Bone* **51**, 353–361.

Hoffmann, A., and Baltimore, D. (2006). Circuitry of nuclear factor kappaB signaling. *Immunol. Rev.* **210**, 171–186.

Hughes, D. E., Dai, A., Tiffee, J. C., Li, H. H., Mundy, G. R., and Boyce, B. F. (1996). Estrogen promotes apoptosis of murine osteoclasts mediated by TGF-beta. *Nat. Med.* **2**, 1132–1136.

Ignasiak, Z., Slawinska, T., Rozek, K., Little, B. B., and Malina, R. M. (2006). Lead and growth status of school children living in the copper basin of south-western Poland: Differential effects on bone growth. *Ann. Hum. Biol.* **33**, 401–414.

Iotsova, V., Caamano, J., Loy, J., Yang, Y., Lewin, A., and Bravo, R. (1997). Osteopetrosis in mice lacking NF-kappaB1 and NF-kappaB2. *Nat. Med.* **3**, 1285–1289.

Jackson, L. W., Cromer, B. A., and Panneerselvamm, A. (2010). Association between bone turnover, micronutrient intake, and blood lead levels in pre- and postmenopausal women, NHANES 1999-2002. *Environ. Health Perspect.* **118**, 1590–1596.

Jakubowski, M. (2011). Low-level environmental lead exposure and intellectual impairment in children–the current concepts of risk assessment. *Int. J. Occup. Med. Environ. Health* **24**, 1–7.

Keeleyside, A. Song, X., Chettle, D., Webber, C. (1996). The lead content of human bones from the 1845 Franklin expedition. *J. Archaeo. Sci.* **23**, 461–465.

Khalil, N., Cauley, J. A., Wilson, J. W., Talbott, E. O., Morrow, L., Hochberg, M. C., Hillier, T. A., Muldoon, S. B., and Cummings, S. R. (2008). Relationship of blood lead levels to incident nonspine fractures and falls in older women: The study of osteoporotic fractures. *J. Bone Min. Res.* **23**, 1417–1425.

Korashy, H. M., and El-Kadi, A. O. (2008). The role of redox-sensitive transcription factors NF-kappaB and AP-1 in the modulation of the Cyp1a1 gene by mercury, lead, and copper. *Free Radic. Biol. Med.* **44**, 795–806.

Kostenuik, P. J., Capparelli, C., Morony, S., Adamu, S., Shimamoto, G., Shen, V., Lacey, D. L., and Dunstan, C. R. (2001). OPG and PTH-(1-34) have additive effects on bone density and mechanical strength in osteopenic ovariectomized rats. *Endocrinology* **142**, 4295–4304.

Kudrin, A. V. (2000). Trace elements in regulation of NF-kappaB activity. *J. Trace Elem. Med. Biol.* **14**, 129–142.

Liu, C. M., Sun, Y. Z., Sun, J. M., Ma, J. Q., and Cheng, C. (2012). Protective role of quercetin against lead-induced inflammatory response in rat kidney through the ROS-mediated MAPKs and NF-kappaB pathway. *Biochim. Biophys. Acta* **1820**, 1693–1703.

Liu, Y., Song, C. Y., Wu, S. S., Liang, Q. H., Yuan, L. Q., and Liao, E. Y. (2013). Novel adipokines and bone metabolism. *Int. J. Endocrinol.* **2013**, 895045.

Monir, A. U., Gundberg, C. M., Yagerman, S. E., van der Meulen, M. C., Budell, W. C., Boskey, A. L., and Dowd, T. L. (2010). The effect of lead on bone mineral properties from female adult C57/BL6 mice. *Bone* **47**, 888–894.

Nash, D., Magder, L. S., Sherwin, R., Rubin, R. J., and Silbergeld, E. K. (2004). Bone density-related predictors of blood lead level among peri- and postmenopausal women in the United States: The Third National Health and Nutrition Examination Survey, 1988-1994. *Am. J. Epidemiol.***160**, 901–911.

Parsons, P. J. (1993). A rapid Zeeman graphite furnace atomic absorption spectrometric method for the determination of lead in blood. *Spectrochim. Acta. A Mol. Biomol. Spectrosc.* **48B**, 925–939.

Pounds, J. G., Long, G. J., and Rosen, J. F. (1991). Cellular and molecular toxicity of lead in bone. *Environ. Health Perspect.* **91**, 17–32.

Rosen, J. F., Chesney, R. W., Hamstra, A., DeLuca, H. F., and Mahaffey, K. R. (1980). Reduction in 1,25-dihydroxyvitamin D in children with increased lead absorption. *N. Engl. J. Med.* **302**, 1128–1131.

Ryan, E. P., Holz, J. D., Mulcahey, M., Sheu, T. J., Gasiewicz, T. A., and Puzas, J. E. (2007). Environmental toxicants may modulate osteoblast differentiation by a mechanism involving the aryl hydrocarbon receptor. *J. Bone Miner. Res.* **22**, 1571–1580.

Segovia-Silvestre, T., Neutzsky-Wulff, A. V., Sorensen, M. G., Christiansen, C., Bollerslev, J., Karsdal, M. A., and Henriksen, K. (2009). Advances in osteoclast biology resulting from the study of osteopetrotic mutations. *Hum. Genet.* **124**, 561–577.

Somervaille, L. J., Chettle, D. R., Scott, M. C., Tennant, D. R., McKiernan, M. J., Skilbeck, A., and Trethowan, W. N. (1988). In vivo tibia lead measurements as an index of cumulative exposure in occupationally exposed subjects. *Br. J. Ind. Med.* **45**, 174–181.

Todd, A. C., Parsons, P. J., Tang, S., and Moshier, E. L. (2001). Individual variability in human tibia lead concentration. *Environ. Health Perspect.* **109**, 1139–1143.

Van den Bossche, J., Bogaert, P., van Hengel, J., Guerin, C. J., Berx, G., Movahedi, K., Van den Bergh, R., Pereira-Fernandes, A., Geuns, J. M., Pircher, H., *et al.* (2009). Alternatively activated macrophages engage in homotypic and heterotypic interactions through IL-4 and polyamine-induced E-cadherin/catenin complexes. *Blood* **114**, 4664–4674.

Wittmers, L. E., Jr., Aufderheide, A. C., Wallgren, J., Rapp, G., Jr., and Alich, A. (1988). Lead in bone. IV. Distribution of lead in the human skeleton. *Arch. Environ. Health* **43**, 381–391.

Yagi, M., Miyamoto, T., Sawatani, Y., Iwamoto, K., Hosogane, N., Fujita, N., Morita, K., Ninomiya, K., Suzuki, T., Miyamoto, K., *et al.* (2005). DC-STAMP is essential for cell-cell fusion in osteoclasts and foreign body giant cells. *J. Exp.Med.* **202**, 345–351.

Yamashita, T., Yao, Z., Li, F., Zhang, Q., Badell, I. R., Schwarz, E. M., Takeshita, S., Wagner, E. F., Noda, M., Matsuo, K., *et al.* (2007). NF-kappaB p50 and p52 regulate receptor activator of NF-kappaB ligand (RANKL) and tumor necrosis factor-induced osteoclast precursor differentiation by activating c-Fos and NFATc1. *J. Biol. Chem.* **282**, 18245–18253.

Yuan, G., Lu, H., Yin, Z., Dai, S., Jia, R., Xu, J., Song, X. and Li, L. (2014). Effects of mixed subchronic lead acetate and cadmium chloride on bone metabolism in rats. *Int. J. Clin. Exp. Med.* **7**, 1378–1385.

Zhu, K. Qiu, J., Ji, H., Yanagisawa, K., Shimanouchi, R., Onda, A., and Kajiyoshi, K. (2010). Crystallographic study of lead-substituted hydroxyapatite synthesized by high temperature mixing method under hydrothermal conditions. *Inorgan. Chim. Acta* **363**, 1785–1790.

Zuscik, M. J., Ma, L., Buckley, T., Puzas, J. E., Drissi, H., Schwarz, E. M., and O'Keefe, R. J. (2007). Lead induces chondrogenesis and alters transforming growth factor-beta and bone morphogenetic protein signaling in mesenchymal cell populations. *Environ. Health Perspect.* **115**, 1276–1282.